

PREPARATION, THERMAL DECOMPOSITION PROCESS AND KINETICS FOR TERBIUM *p*-METHOXYBENZOATE TERNARY COMPLEX WITH 1,10-PHENANTHROLINE

J.-J. Zhang^{1*}, R.-F. Wang², S.-P. Wang², H.-M. Liu³, J.-B. Li¹, J.-H. Bai⁴ and N. Ren²

¹Experimental Center, Hebei Normal University, Shijiazhuang 050016, P. R. China

²College of Chemistry, Hebei Normal University, Shijiazhuang 050091, P. R. China

³College of Chemistry and Pharmaceutical Engineering, Hebei University of Science and Technology, Shijiazhuang 050018, P. R. China

⁴Department of Computer, Hebei Normal College of Science and Technology, Qinhuangdao 066600, P. R. China

The complex of $[\text{Tb}_2(p\text{-MOBA})_6(\text{PHEN})_2]$ ($p\text{-MOBA}=\text{C}_8\text{H}_7\text{O}_3$, p -methoxybenzoate; $\text{PHEN}=\text{C}_{12}\text{H}_8\text{N}_2$, 1,10-phenanthroline) was prepared and characterized by elemental analysis and IR spectroscopy. The thermal behavior of $\text{Tb}_2(p\text{-MOBA})_6(\text{PHEN})_2$ in a static air atmosphere was investigated by TG-DTG, DTA, SEM and IR techniques. By the kinetic method of processing thermal analysis data put forward by Malek *et al.*, it is defined that the kinetic model for the first-step thermal decomposition is SB(m,n). The activation energy E for this step reaction is $140.92 \text{ kJ mol}^{-1}$, the enthalpy of activation ΔH^\ddagger is $136.06 \text{ kJ mol}^{-1}$, the Gibbs free energy of activation ΔG^\ddagger is $145.16 \text{ kJ mol}^{-1}$, the entropy of activation ΔS^\ddagger is $-15.53 \text{ J mol}^{-1}$, and the pre-exponential factor $\ln A$ is 29.26. The lifetime equation at mass loss of 10% was deduced as $\ln \tau = -28.72 + 1.943 \cdot 10^4/T$ by isothermal thermogravimetric analysis.

Keywords: lifetime, non-isothermal kinetics, p -methoxybenzoate, terbium complex, thermal decomposition

Introduction

The rare-earth carboxylic acid complexes have many special structure and interesting spectroscopic properties, which is of great interest in extraction, separation, germicide, catalysis, luminescence and functional materials. The preparation, structure and thermal properties of some rare-earth carboxylic acid complex have been studied [1–19]. In this paper, we have prepared the complex of terbium p -methoxybenzoate with 1,10-phenanthroline and discussed its thermal decomposition procedure by TG-DTG, DTA, SEM and IR techniques and the corresponding non-isothermal kinetics in terms of the Malek method [20, 21]. The lifetime equation at mass loss of 10% was obtained by isothermal thermogravimetric analysis. This has some directive significance to the determination of the stability of the title compound in different temperatures, and also provides basis for the preparation of the composite luminous materials with good thermal stability.

Experimental

Preparation of complex $[\text{Tb}_2(p\text{-MOBA})_6(\text{PHEN})_2]$

A stoichiometric amount of p -methoxybenzoic acid was dissolved in 95% $\text{C}_2\text{H}_5\text{OH}$ and its pH was con-

trolled in a range of 6–7 with 1 mol L^{-1} NaOH solution. A quantitative amount 1,10-phenanthroline was also dissolved in 95% $\text{C}_2\text{H}_5\text{OH}$. The two solutions were mixed, and added dropwise into the TbCl_3 solution prepared by dissolving $\text{TbCl}_3 \cdot 6\text{H}_2\text{O}$ in 95% $\text{C}_2\text{H}_5\text{OH}$. The mixture was heated under reflux with stirring for a few hours. The white precipitate was formed.

Apparatus and measurements

The carbon, hydrogen and nitrogen analyses were made using a Carlo Erba model 1106 elemental analyzer. The metal content was assayed using EDTA titration method.

Infrared spectra were recorded as KBr discs on Bio-Rad FTS-135 spectrometer, between 4000 and 400 cm^{-1} .

The TG and DTG experiments for the title compounds were performed using a Perkin Elmer's TGA7 thermogravimetric analyzer. The heating rate used were 3, 5, 7, $10^\circ\text{C min}^{-1}$ from ambient to 700°C and the sample size was $(3.6 \pm 0.2) \text{ mg}$. Air was used as a static atmosphere.

The DTA curve was carried out on a Perkin Elmer DTA 1700 with a system 7/4 controller. The sample mass was 2.2 mg. The heating rate used were 5°C min^{-1} . Air was used as a static atmosphere.

* Author for correspondence: jjzhang6@sohu.com

Results and discussion

Elemental analyses and infrared spectra

Analytical results for the complex compared with theoretical calculation results from the proposed formulate are given in Table 1. It can be seen that the experimental data agree with values of theoretical calculation.

Table 1 Elemental analyses of the complex

Complex [Tb ₂ (<i>p</i> -MOBA) ₆ (PHEN) ₂]	Mass fraction/%			
	C	H	N	Tb
Theoretical values	54.54	3.69	3.54	20.06
Experimental data	54.20	3.84	3.32	20.35

Frequencies of characteristic absorption bands in IR spectra (cm⁻¹) for ligands and complex are listed in Table 2. The IR spectra of the complex show that the absorption valence band of the C=O group, $\nu_{C=O}$ at 1685 cm⁻¹, disappear, whereas the bands of the asymmetric vibrations $\nu_{as(COO^-)}$ at 1605 cm⁻¹ and of the symmetric vibrations $\nu_{s(COO^-)}$ at 1417 cm⁻¹ are apparent. The values of the splitting for the absorption bands of the valency vibration $\nu_{as(COO^-)}$ and $\nu_{s(COO^-)}$ ($\Delta\nu = \nu_{as} - \nu_s$) is very high ($\Delta\nu = 188$ cm⁻¹). The IR spectra of the complex show that the absorption valency band of the $\nu_{C=N}$ at 1644 cm⁻¹ are observed to move lower wavenumber. The spectroscopy data suggest that the Tb³⁺ is coordinated with N atoms of 1,10-phenanthroline and O atoms of *p*-methoxybenzoate [22, 23].

Thermogravimetric decomposition data

Thermal analytical data measured at $\beta = 5^\circ\text{C min}^{-1}$ for title compound are presented in Table 3. The percent-

Table 2 Frequencies of characteristic absorption bands in IR spectra (cm⁻¹) for ligands, complex and some intermediate products of the thermal decomposition

Compounds	$\nu_{C=N}$	$\nu_{C=O}$	$\nu_{as(COO^-)}$	$\nu_{s(COO^-)}$	$\Delta\nu = \nu_{as} - \nu_s$
PHEN	1644	—	—	—	—
<i>p</i> -MOBA	—	1685	—	—	—
Tb ₂ (<i>p</i> -MOBA) ₆ (PHEN) ₂	1639	—	1605	1417	188
Intermediate (Tb ₂ (<i>p</i> -MOBA) ₆)	—	—	1608	1422	186
End product (Tb ₄ O ₇)	—	—	—	—	—

Table 3 Thermal decomposition data for Tb₂(*p*-MOBA)₆(PHEN)₂ from TG and DTG analysis ($\beta = 5^\circ\text{C min}^{-1}$)

Stage	$T_{\text{range}}/^\circ\text{C}$	DTG peak $T/^\circ\text{C}$	Mass loss/%		Probable composition of expelled groups	Intermediate
			TG	Theory		
I	252.83–354.08	310.48	23.29	22.74	–2PHEN	[Tb ₂ (<i>p</i> -MOBA) ₆]
II	354.08–486.28	418.77–451.12	28.34	28.60	–3 <i>p</i> -MOBA	[Tb ₂ (<i>p</i> -MOBA) ₃]
III	486.28–659.26	524.25–605.82	24.58	25.07	–C ₂₄ H ₂₁ O _{5.5}	Tb ₄ O ₇

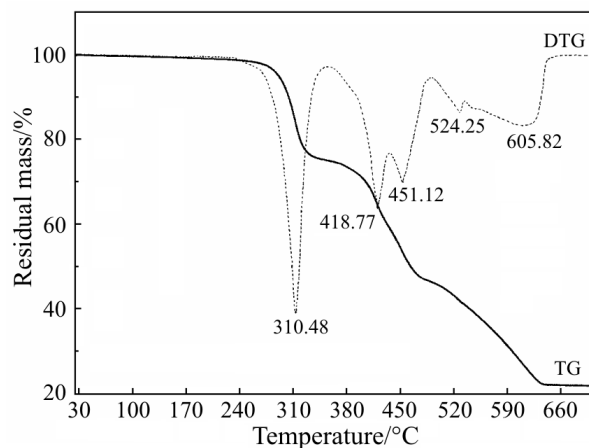


Fig. 1 TG-DTG curves of Tb₂(*p*-MOBA)₆(PHEN)₂ (heating rate of 5°C min⁻¹)

ages of mass loss and probable composition of the expelled groups are also given. TG and DTG curves of Tb₂(*p*-MOBA)₆(PHEN)₂ are shown in Fig. 1. The results of thermal analysis indicate that the thermal decomposition of Tb₂(*p*-MOBA)₆(PHEN)₂ begins at 252.83°C and terminated at 659.26°C. The thermal decomposition process of Tb₂(*p*-MOBA)₆(PHEN)₂ can be divided into three stages, as was observed by the DTG curve (Fig. 1). The first stage starts from 252.83 to 354.08°C with a mass loss 23.29% which corresponds to the loss of 2 mol C₁₂H₈N₂ (theoretical mass loss is 22.74%). The IR spectra of the residue at 354°C shows that the absorption band of C=N disappear at 1639 cm⁻¹. The SEM pictures show that the form of the complex changed from a smooth-surface cylinder to a crackled cylinder (Fig. 2). The second stage in the degradation occurs from 354.08 to 486.28°C. Actually, from DTG curve (Fig. 1), this

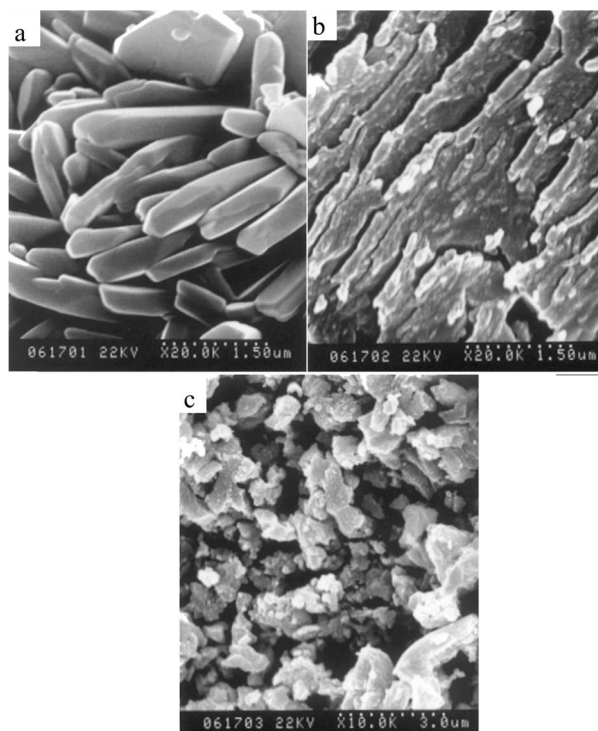


Fig. 2 Scanning electron micrographs of $\text{Tb}_2(p\text{-MOBA})_6(\text{PHEN})_2$: a – RT; b – 354°C and c – 659°C

stage includes two steps but there is no clear plateau in the TG curve, namely the intermediate product is unstable, which continues to lose mass with rising temperature until the formation of $[\text{Tb}_2(p\text{-MOBA})_3]$ with a mass loss of 28.34% (theoretical mass loss = 28.60%). The third-stage degradation temperature is in the range of 486.28–659.26°C with the mass loss of 24.58%, in which $\text{C}_{24}\text{H}_{21}\text{O}_{5.5}$ are removed with theoretical mass loss of 25.07%. And in this stage degradation also includes two steps. The bands of the asymmetric vibrations $\nu_{\text{as}(\text{COO}^-)}$ at 1608 cm^{-1} and of the symmetric vibration $\nu_{\text{s}(\text{COO}^-)}$ at 1422 cm^{-1} for the title complex heated 659°C disappeared. The SEM pictures for the product obtained at 659°C are also completely different from that of the complex at room temperature. The formation of above-mentioned products from $[\text{Tb}_2(p\text{-MOBA})_6(\text{PHEN})_2]$ should be accomplished with a theoretical overall mass loss of 76.41%. It was in agreement with the experimental value of 76.21%.

The DTA curve recorded in the range of 25–700°C at a heating rate of 5°C min^{-1} for the title compound is given in Fig. 3. One endothermic peak and two exothermic peaks are apparent. The first peak (endothermic) appears between 278 to 294°C

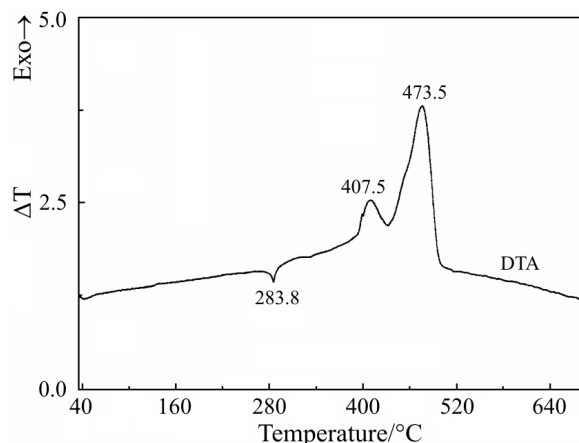


Fig. 3 DTA curve of $\text{Tb}_2(p\text{-MOBA})_6(\text{PHEN})_2$ (heating rate of 5 min^{-1})

representing the loss of 2 mol *PHEN* from the $[\text{Tb}_2(p\text{-MOBA})_6(\text{PHEN})_2]$. The second peak (exothermic) is found between 385–431°C, representing the loss of 3 *p*-MOBA from the $[\text{Tb}_2(p\text{-MOBA})_6]$. The third peak (exothermic) which represents the loss of one molecule of $\text{C}_{24}\text{H}_{21}\text{O}_{5.5}$ from $[\text{Tb}_2(p\text{-MOBA})_3]$ to yield Tb_4O_7 , is observed between 431 and 504°C. From the above analysis, the thermal decomposition process of $[\text{Tb}_2(p\text{-MOBA})_6(\text{PHEN})_2]$ may be expressed by Scheme 1.

Kinetics of the first decomposition stage

In the present work, the Malek method [20, 21] was applied to the first decomposition processes of $[\text{Tb}_2(p\text{-MOBA})_6(\text{PHEN})_2]$. The activation energy E is the most important factor for determination of the function $f(\alpha)$ [20], so in the condition of not touching the kinetic function, we calculated values of E of the first thermal decomposition step by Ozawa equation [24]. The results are listed in Table 4, from which it can be seen that the average values of E is $140.92\text{ kJ mol}^{-1}$. This value was used to calculate function $Y(\alpha)$ and $Z(\alpha)$. The experimental data of T , α and $d\alpha/dt$ can be obtained from TG-DTG curves. Function $Y(\alpha)$ and $Z(\alpha)$ can be obtained by the transformation of experimental data and activation energy E to the following equations [20]

$$Y(\alpha) = (d\alpha/dt)e^x \quad (1)$$

$$Z(\alpha) = \Pi(x)(d\alpha/dt)T/\beta \quad (2)$$

where $x = E/RT$, $\Pi(x)$ expression of temperature integral, $\Pi(x) = (x^3 + 18x^2 + 88x + 96)/(x^4 + 20x^3 + 120x^2 + 240x + 120)$. Figures 4 and 5 show the dependence of $Y(\alpha)$ and $Z(\alpha)$ on α , respectively. From Fig. 4 it can be seen that func-



Scheme 1

Table 4 The activation energy for the first-stage decomposition of $[\text{Tb}_2(p\text{-MOBA})_6(\text{PHEN})_2]$ obtained by Ozawa method

No.	α	Temperature/K				$E/\text{kJ mol}^{-1}$	$E^{\circ}/\text{kJ mol}^{-1}$	r
		$3^{\circ}\text{C min}^{-1}$	$5^{\circ}\text{C min}^{-1}$	$7^{\circ}\text{C min}^{-1}$	$10^{\circ}\text{C min}^{-1}$			
1	0.10	549.93	557.88	562.15	567.66	168.70	140.92	0.9988
2	0.15	555.50	563.47	567.72	574.17	164.65		0.9985
3	0.20	560.15	568.12	572.37	578.81	167.46		0.9985
4	0.30	565.72	573.71	577.95	585.32	163.24		0.9968
5	0.40	570.37	578.36	582.60	589.97	165.71		0.9963
6	0.50	574.08	582.09	586.32	594.61	160.76		0.9945
7	0.55	575.91	583.95	589.11	597.40	154.04		0.9959
8	0.60	576.87	584.88	590.96	600.19	141.63		0.9939
9	0.70	579.66	587.67	596.54	605.77	125.39		0.9929
10	0.80	582.44	592.33	603.05	614.13	105.41		0.9939
11	0.85	583.37	595.12	607.70	619.71	92.86		0.9955
12	0.90	585.23	598.84	614.20	627.14	81.18		0.9954

^aAverage value of E

tion $Y(\alpha)$ has a clear maximum when α is more than zero, which indicates that the kinetic model of the first thermal decomposition step of title complex is JMA($n > 1$) or SM(m, n). Figure 5 shows $Z(\alpha)$ has a clear maximum, which is consistent with the fact that $Z(\alpha)$ function has a maximum at α_p^{∞} for all the kinetic models summarized in Tables 1 and 2 in [20]. In order to obtain the accurate values of α_m and α_p^{∞} , at which function $Y(\alpha)$ and $Z(\alpha)$ have a maximum respectively, we used Mathematica 4.1 software for the fitting of the curves $Y(\alpha)-\alpha$ and $Z(\alpha)-\alpha$. It is found that the equation obtained by five time-fitting is the most accurate because the experimental data in the curve after five times fitting are the most. The fitted equations at various heating rates are described as follows in Scheme 2.

The values of α_m and α_p^{∞} at various heating rate can be obtained by derivation of above equations (Table 5). From Table 5 it can be seen that the values of α_m at various heating rate are all more than zero and less

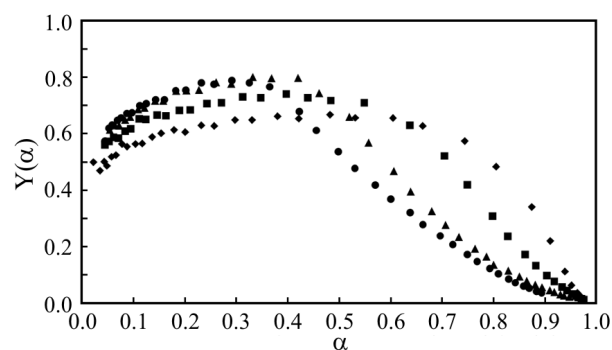


Fig. 4 Normalized $Y(\alpha)$ function corresponding to the first step decomposition kinetic data measured at various heating rates for $[\text{Tb}_2(p\text{-MOBA})_6(\text{PHEN})_2]$ ($\beta/^{\circ}\text{C min}^{-1}$: \blacklozenge - 3, \blacksquare - 5, \blacktriangle - 7, \bullet - 10)

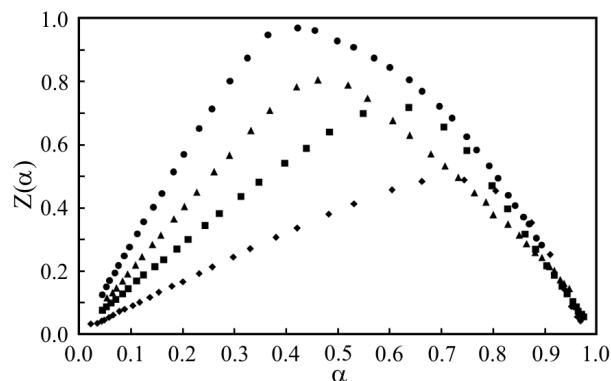


Fig. 5 Normalized $Z(\alpha)$ function corresponding to the first step decomposition kinetic data measured at various heating rates for $[\text{Tb}_2(p\text{-MOBA})_6(\text{PHEN})_2]$ ($\beta/^{\circ}\text{C min}^{-1}$: \blacklozenge - 3, \blacksquare - 5, \blacktriangle - 7, \bullet - 10)

than those of α_p at various heating rate, and values of α_p^{∞} at various heating rate are not equal to 0.632. By combining with the Fig. 4 in [20] the kinetic model of the first thermal decomposition step can be determined to be SB(m, n). The kinetic exponents m and n were calculated from the following equations [20]:

$$\ln[(d\alpha/dt)e^x] = \ln A + n \ln[\alpha_p(1-\alpha)] \quad (3)$$

Table 5 The characteristic feature of the functions $Y(\alpha)$ and $Z(\alpha)$

$\beta/^{\circ}\text{C min}^{-1}$	Shape of $Y(\alpha)$	α_m	α_p^{∞}	α_p
3	Convex	0.5203	0.7129	0.5541
5	Convex	0.4319	0.5984	0.5496
7	Convex	0.3198	0.4736	0.4629
10	Convex	0.2624	0.4496	0.3992

$$\beta=3^{\circ}\text{C min}^{-1}$$

$$Y(\alpha)=-0.426088+1.91654\alpha-7.05615\alpha^2+13.227\alpha^3-10.9076\alpha^4+2.26345\alpha^5$$

$$Z(\alpha)=0.0078427+0.731288\alpha+0.924539\alpha^2-4.44634\alpha^3+8.30817\alpha^4-5.66084\alpha^5$$

$$\beta=5^{\circ}\text{C min}^{-1}$$

$$Y(\alpha)=0.45952+2.65082\alpha-12.771\alpha^2+33.6457\alpha^3-42.3431\alpha^4+18.3799\alpha^5$$

$$Z(\alpha)=-0.0331766+2.60673\alpha-10.0416\alpha^2+32.2859\alpha^3-43.4091\alpha^4+18.6141\alpha^5$$

$$\beta=7^{\circ}\text{C min}^{-1}$$

$$Y(\alpha)=0.633361-0.680805\alpha+12.5452\alpha^2-38.0939\alpha^3+38.2705\alpha^4-12.6562\alpha^5$$

$$Z(\alpha)=0.133141-0.937341\alpha+19.1012\alpha^2-46.9787\alpha^3+41.6674\alpha^4-12.9158\alpha^5$$

$$\beta=10^{\circ}\text{C min}^{-1}$$

$$Y(\alpha)=0.563407+0.710526\alpha+6.64915\alpha^2-33.3292\alpha^3+42.9404\alpha^4-17.6845\alpha^5$$

$$Z(\alpha)=0.0795247+0.557817\alpha+18.8848\alpha^2-58.5372\alpha^3+62.9964\alpha^4-24.1897\alpha^5$$

Scheme 2

$$m=pn \quad (4)$$

$$p=\alpha_m/(1-\alpha_m) \quad (5)$$

and the results are listed in Table 6. The pre-exponential factor A in the first thermal decomposition step were calculated from the following equations:

$$A=-\beta x_p \exp(x_p) / [T_p f'(\alpha_p)] \quad (6)$$

where $f'(\alpha_p) = (df(\alpha_p)/d\alpha)$ and the results are listed in Table 6.

Table 6 Kinetic parameters and mechanism

$\beta/$ $^{\circ}\text{C min}^{-1}$	KM ^b	m	n	$\ln A/$ s^{-1}	$E/$ kJ mol^{-1}
3	SB	1.1470	1.0575	30.54	140.92
5	SB	0.7063	0.9290	28.99	
7	SB	0.2944	0.6262	28.76	
10	SB	0.1429	0.4016	28.76	

^bkinetic model

The thermodynamic parameters of activation can be calculated from the equations [25, 26]:

$$A \exp(-E/RT) = \nu \exp(-\Delta G^{\ddagger}/RT) \quad (7)$$

$$\Delta H^{\ddagger} = E - RT \quad (8)$$

$$\Delta G^{\ddagger} = \Delta H^{\ddagger} - T\Delta S^{\ddagger} \quad (9)$$

where ν is the Einstein vibration frequency, ΔG^{\ddagger} is the Gibbs free enthalpy of activation, ΔH^{\ddagger} is the enthalpy of activation, ΔS^{\ddagger} is entropy of activation. The values of entropy, enthalpy and the Gibbs free

energy of activation at the peak temperature obtained on the basis of Eqs (7)–(9) are listed in Table 7.

Table 7 The thermodynamic parameters of title compound

$\beta/$ $^{\circ}\text{C min}^{-1}$	$\Delta H^{\ddagger}/$ kJ mol^{-1}	$\Delta G^{\ddagger}/$ kJ mol^{-1}	$\Delta S^{\ddagger}/$ $\text{J mol}^{-1}\text{K}^{-1}$	$T_p/$ K
3	136.11	138.90	-4.83	578.98
5	136.07	146.45	-17.79	583.63
7	136.06	147.59	-19.72	585.04
10	136.01	147.69	-19.79	589.97

Lifetime

Dakin [13] has proposed and proved that the general lifetime formula of materials is

$$\ln \tau = a/T + b \quad (10)$$

where τ is the lifetime at temperature $T(\text{K})$, a and b are constant. In this paper, the mass loss of 10% lifetime was measured by isothermal temperature TG at 230, 245, 260 and 275°C and listed in Table 8. By substituting the value in Table 8 into Eq. (10), the constant a , b and linear correlation coefficients r were obtained by the linear least squares method. The lifetime equation is $\ln \tau = -28.72 + 1.943 \cdot 10^4/T$. Linear correlation coefficients r is 0.9958. The lifetime values at various temperatures were calculated from equation and were listed in Table 9.

Table 8 The lifetime of the $[\text{Tb}_2(p\text{-MOBA})_6(\text{PHEN})_2]$ by isothermal temperature TG

$T/^\circ\text{C}$	$\tau_{10\%}/\text{min}$	$T/^\circ\text{C}$	$\tau_{10\%}/\text{min}$
230	302.00	260	43.25
245	115.54	275	12.29

Table 9 The lifetime values of the $[\text{Tb}_2(p\text{-MOBA})_6(\text{PHEN})_2]$ at various temperatures

$T/^\circ\text{C}$	T/K	τ/min	$T/^\circ\text{C}$	T/K	τ/min
50	323.15	$7.272 \cdot 10^{11}$	200	473.15	3831
75	348.15	$9.696 \cdot 10^9$	230	503.15	302 ^a
100	373.15	$2.305 \cdot 10^8$	245	518.15	115.54 ^a
125	398.15	$8.766 \cdot 10^6$	260	533.15	43.29 ^a
150	423.15	$4.905 \cdot 10^5$	275	548.15	12.29 ^a
175	448.15	$3.786 \cdot 10^4$	300	573.15	2.962

^aResults determined from lifetime tests

Conclusions

There are three steps in the thermal decomposition of $[\text{Tb}_2(p\text{-MOBA})_6(\text{PHEN})_2]$. In the first step, the activation energy E is $140.92 \text{ kJ mol}^{-1}$, the enthalpy of activation ΔH^\ddagger is $136.06 \text{ kJ mol}^{-1}$, the Gibbs free energy of activation ΔG^\ddagger is $145.16 \text{ kJ mol}^{-1}$, the entropy of activation ΔS^\ddagger is $-15.53 \text{ J mol}^{-1}$, the pre-exponential factor $\ln A$ is 29.26 and the kinetic model was determined to be SB(m, n) model. The lifetime equation at mass loss of 10% was deduced as $\ln \tau = -28.72 + 1.943 \cdot 10^4/T$ by isothermal thermogravimetric analysis.

Acknowledgements

This project was supported by the Natural Science Foundation of Hebei Province and Hebei Education Department.

References

- 1 Y. Zhang, L. P. Jin and S. Z. Lü, Chinese, J. Inorg. Chem. (in Chinese), 13 (1997) 280.

- 2 R. F. Wang, L. S. Li, L. P. Jin and S. Z. Lu, J. Rare Earths, 16 (1998) 149.
- 3 L. P. Jin, R. F. Wang and L. S. Li. Polyhedron, 18 (1999) 487.
- 4 L. P. Jin, M. Z. Wang, G. L. Cai, S. X. Liu and J. L. Huang, Science in China (Series B), 38 (1995) 1.
- 5 R. F. Wang, L. P. Jin, L. S. Li, S. Z. Lu and J. H. Zhang, J. Coord. Chem., 47 (1999) 279.
- 6 L. P. Jin, R. F. Wang and L. S. Li, J. Rare Earths, 14 (1996) 161.
- 7 R. F. Wang, S. P. Wang, S. K. Shi and J. J. Zhang, J. Coord. Chem., 55 (2002) 215.
- 8 J. J. Zhang, R. F. Wang, J. B. Li, H. M. Liu and H. F. Yang, J. Therm. Anal. Cal., 62 (2000) 747.
- 9 J. J. Zhang, R. F. Wang, J. L. Zhao, L. P. Mo, X. L. Zhai and L. G. Ge, Rare Metals, 18 (1999) 182.
- 10 J. J. Zhang, R. F. Wang, X. L. Zhai, J. L. Zhao, H. F. Yang and L. P. Mo, Chinese J. Inorg. Chem., 16 (2000) 103.
- 11 H. F. Yang, J. J. Zhang and R. F. Wang, Rare Metals, 20 (2001) 133.
- 12 J. J. Zhang, R. F. Wang, J. B. Li and H. M. Liu, J. Therm. Anal. Cal., 65 (2001) 241.
- 13 J. J. Zhang and R. F. Wang, Chinese J. Anal. Chem. (in Chinese), 29 (2001) 1209.
- 14 J. J. Zhang, R. F. Wang and H. M. Liu, J. Therm. Anal. Cal., 66 (2001) 431.
- 15 R. F. Wang, S. P. Wang and J. J. Zhang, J. Mol. Struct., 648 (2003) 151.
- 16 J. J. Zhang, R. F. Wang and S. P. Wang, J. Therm. Anal. Cal., 73 (2003) 977.
- 17 B. Czajka, B. Bocian and W. Ferenc, J. Therm. Anal. Cal., 67 (2002) 631.
- 18 W. Ferenc and A. Walków-Dziewulska, J. Therm. Anal. Cal., 74 (2003) 511.
- 19 W. Ferenc and A. Walków-Dziewulska, J. Therm. Anal. Cal., 70 (2002) 949.
- 20 J. Malek, Thermochim. Acta, 200 (1992) 257.
- 21 J. Malek and V. Smrcka, Thermochim. Acta, 186 (1991) 153.
- 22 R. F. Wang, L. P. Jin and M. Z. Wang, Acta Chimica Sinica (in Chinese), 53 (1995) 39.
- 23 R. F. Wang, J. J. Zhang and L. P. Jin, Chinese J. Spectroscopy Laboratory (in Chinese), 13 (1996) 1.
- 24 T. Ozawa, J. Thermal Anal., 38 (1965) 1881.
- 25 J. Straszko, M. Olstak-Humienik and J. Mozejko, Thermochim. Acta, 292 (1997) 145.
- 26 M. Olstak-Humienik and J. Mozejko, Thermochim. Acta, 344 (2000) 73.

Received: July 29, 2003

In revised form: July 22, 2004